

Guaranteed Discovery of Controllable Latent States with Multi-Step Inverse Models

Alex Lamb^{1,*}, Riashat Islam^{1,2}, Yonathan Efroni¹, Aniket Didolkar³
Dipendra Misra¹, Dylan Foster¹, Lekan Molu¹, Rajan Chari¹
Akshay Krishnamurthy¹, John Langford^{1,*}

¹Microsoft Research NYC, New York, USA

² School of Computer Science, McGill University, Montreal, Canada

³ Department of Computer Science, University of Montreal, Montreal, Canada

Corresponding Authors. E-mails: lambalex@microsoft.com, jcl@microsoft.com

July 19, 2022

Abstract

A person walking along a city street who tries to model all aspects of the world would quickly be overwhelmed by a multitude of shops, cars, and people moving in and out of view, following their own complex and inscrutable dynamics. Exploration and navigation in such an environment is an everyday task, requiring no vast exertion of mental resources. Is it possible to turn this fire hose of sensory information into a minimal latent state which is necessary and sufficient for an agent to successfully act in the world? We formulate this question concretely, and propose the Agent-Controllable State Discovery algorithm (*AC-State*), which has theoretical guarantees and is practically demonstrated to discover the *minimal controllable latent state* which contains all of the information necessary for controlling the agent, while fully discarding all irrelevant information. This algorithm consists of a multi-step inverse model (predicting actions from distant observations) with an information bottleneck. *AC-State* enables localization, exploration, and navigation without reward or demonstrations. We demonstrate the discovery of controllable latent state in three domains: localizing a robot arm with distractions (e.g., changing lighting conditions and background), exploring in a maze alongside other agents, and navigating in the Matterport house simulator.

Main

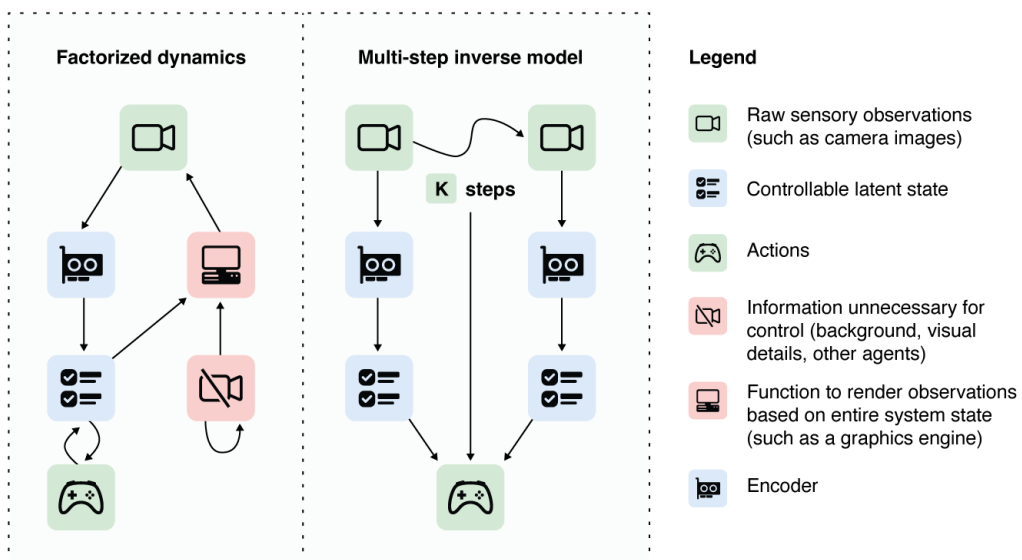
Several scientific fields, ranging from classical mechanics, chemistry and evolution, to sub-fields of medicine have parsimonious representations for encapsulating how a system (or

an agent) interacts with the world. For example, consider a world consisting of a robot arm agent that is manipulating objects using feedback from a camera-based sensor. The agent’s high-dimensional camera observation intertwines information which the agent controls and many distractors from exogenous sources such as lighting conditions. A parsimonious representation enables efficiency for many applications by capturing essential information such as the joint angles between the arm’s links and excluding visual details unrelated to the agent’s dynamics. We define *controllable latent state* as the parsimonious representation which includes only information which either can be changed by the agent (such as an object on the table that can be manipulated by the arm) or information which affects the agent’s actions (e.g., an obstacle blocking the robot arm’s motion). How can we discover this controllable latent state from observations? We introduce the Agent-Controllable (AC-State) algorithm which provably guarantees discovery of the controllable latent state from observations, which excludes all aspects of the observations unnecessary for control. AC-State learns an encoder f that maps a given observation x to the corresponding controllable latent state $f(x)$. This is accomplished by optimizing a novel objective using an expressive model class such as deep neural networks (1).

The controllable latent state enables an agent to efficiently localize, explore, and navigate itself within the world. As an example, a household robot vacuum must cover the entire area of the house to provide effective cleaning. This can be accomplished quickly using AC-State. For example, the robot can localize within the controllable latent space using the latent state encoder learned by AC-State, plan to reach a specific room and cover the floor there, then execute the plan in the real-world. Since the controllable latent state excludes irrelevant noise in the house, such as changes in light conditions during the day, the corresponding latent space is small. A smaller latent space enables efficient learning and planning.

Learning controllable latent state can be more formally characterized by considering a discrete-time dynamical system where the observations $x_1, x_2, x_3, \dots, x_T$ evolve according to the observed dynamics, which we write as the conditional probability distribution: $T(x_{t+1}|x_t, a_t)$. The selection of a_t as a function of x_t is the policy, which can be learned or hand-designed. The latent dynamics can then be factorized as $T(s_{t+1} | s_t, a_t)T(e_{t+1} | e_t)$, where s is the controllable latent state, and e is the exogenous information in the observation space, which is irrelevant for control (2). Successful discovery of controllable latent state entails only learning a model of $T(s_{t+1} | s_t, a_t)$ and how to encode s , while not learning anything about $T(e_{t+1} | e_t)$ or how to encode e .

To build further intuition for the concept of controllable latent state, we can consider video games. A video game typically consists of a factorized game engine (which receives player input and updates a game state) and a graphics engine. Modern video game programs are often dozens of gigabytes, with nearly all of the space being used to store high-resolution textures, audio files, and other assets. A full generative model $T(x_{t+1}|x_t, a_t)$ would need to use most of its capacity to model these high-resolution assets. On the other hand, the core gameplay engine necessary for characterizing the controllable latent dynamics $T(s_{t+1} | s_t, a_t)$ takes up only a small fraction of the overall game program’s size, and



AC-State uses observations and actions from an environment and discovers the encoder to discover controllable latent state without having to learn anything about the exogenous noise or how the observation is rendered .

Figure 1: AC-State (right) is able to recover the controllable latent state of the factorized dynamics (left).

thus may be much easier to model¹. Successful reinforcement learning projects for modern video games such as AlphaStar (Starcraft 2) and OpenAI Five (Dota 2) take advantage of this by learning on top of internal game states rather than raw visual observations (3, 4). In the real-world, there is no internal game state that we can extract. The controllable latent state must be learned from experience.

Deep learning architectures can be optimized for a wide range of differentiable objective functions. Our key question is: what is an objective for provably learning controllable latent state which is compatible with deep learning? At issue is finding parsimonious representations which are sufficient for control of a dynamical system given observations from rich sensors (such as high-resolution videos) while discarding irrelevant details. Approaches such as optimal state estimation (5), system identification (6), and simultaneous localization and mapping (7, 8) achieve parsimonious state estimation for control, yet require more domain expertise and design than is desirable. Previous learning-based approaches fail to capture the full controllable latent state or fail to exclude all irrelevant information. Reinforcement learning approaches that employ autoencoders (9) or contrastive learning to capture the latent state from rich sensors often capture noise components². Generative latent models of the world dynamics can be separated into controllable and exogenous latent state, yet these require either learning a full generative model (10) or access to encoders for all of the relevant latent factors (11). In both of these cases, the transition dynamics are learned over the entire latent state, not just the controllable latent state.

Approaches that involve predicting future latent states from past latent states have achieved good performance but have no theoretical guarantee that the latent state will capture the full controllable latent state (12–14). Despite that limitation, these approaches can successfully ignore exogenous noise. Reward-based bisimulation (15), can filter irrelevant information from the latent state, but is dependent on access to a reward signal. Deep reinforcement learning based on reward optimization (16) often struggles with sample complexity when the reward is sparse and fails completely when the reward is absent. In contrast, approaches based on one-step inverse models (17) are widely used in practice (18, 19). In theory, these inverse models can fail to capture the full controllable latent dynamics (2, 20), while combining them with an autoencoder (21) inherits the weaknesses of that approach.

The controllable latent state should preserve information about the interaction between states and actions while discarding irrelevant details. The proposed objective (Agent-Controllable State or *AC-State*) accomplishes this by generalizing one-step inverse dynamics (17) to multiple steps with an information bottleneck (Figure 1). This multi-step inverse model predicts the first action taken to reach a controllable latent state k steps in the future:

¹The controllable latent state and their dynamics is generally even more compact than the game state, which itself may have exogenous noise such as unused or redundant variables.

²Consider a divided freeway, where cars travel on opposing sides of the lane. For this situation, autoencoder or contrastive learning objectives (commonly referred to as self-supervised learning) produce distinct latent states for every unique configuration of cars on the other side of the lane divider. For example, an autoencoder or generative model would learn to predict the full configuration and visual details of all the cars, even those which cannot interact with the agent.

$$\mathcal{L}_{\text{AC-State}}(f) = - \mathbb{E}_{\substack{t \sim U(0,T), \\ k \sim U(1,K)}} \log \mathbb{P}(a_t | f(x_t), f(x_{t+k}); k), \quad (1)$$

$$G = \arg \min_{f \in \mathcal{F}} \mathcal{L}_{\text{AC-State}}(f), \quad (2)$$

$$\hat{f} \in \arg \min_{f \in G} \text{Range}(f). \quad (3)$$

We optimize the parameters of an encoder model $f : \mathbb{R}^n \rightarrow \{1, \dots, \text{Range}(f)\}$ which maps from an n -dimensional continuous observation to a finite latent state with output range of size $\text{Range}(f)$, an integer number. The set \mathcal{F} represents all mappings achievable by the model. The multi-step inverse objective $\mathcal{L}_{\text{AC-State}}$ predicts the action a_t from the observation just before the action a_t is taken and an observation collected k steps in the future. The action step t is sampled uniformly over all of the T collected samples while the prediction horizon k is sampled uniformly from 1 to K .

The controllable latent state is guaranteed to be one of the optimal solutions for the multi-step inverse objective $\mathcal{L}_{\text{AC-State}}$, while other solutions may fail to remove irrelevant information. The controllable latent state is uniquely achievable by also finding the lowest capacity f which minimizes the objective. To further abstract the state, We combine two mechanisms which are widely used in the deep learning literature to restrict the information capacity in f . We first pass the hidden state at the end of the network through a gaussian variational information bottleneck (22), which reduces the mutual information between x and the representation. We then apply vector quantization (23) which yields a discrete latent state. While either of these could be used on their own, we found that adding the gaussian mutual information objective eased discovery of parsimonious discrete representations. In addition to optimizing the objective and restricting capacity, the actions taken by the agent are also important for the success of `AC-State`, in that they must achieve high coverage of the controllable state space and not depend on the exogenous noise. This is satisfied by a random policy or a policy which depends on $\hat{f}(x_t)$ and achieves high coverage. The `AC-State` objective enjoys provable asymptotic success (see supplementary materials) in discovering the controllable latent state.

Intuitively, the `AC-State` objective encourages the latent state to keep information about the long-term effect of actions, which requires storing all information about how the actions affect the world. At the same time, the `AC-State` objective never requires predicting information about the observations themselves, so it places no value on representing aspects of the world which are unrelated to the agent.

The result of training with `AC-State` is a discrete graph where there is a node for every controllable latent state with edges representing actions leading to a state-action node from which weighted outcome edges lead back to controllable latent state nodes. We estimate the transition probabilities in this controllable latent space by using counts to estimate $T(s_{t+1}|s_t, a_t)$. Once this controllable latent state and associated transition distribution is estimated, we can directly measure how correct and how parsimonious these dynamics are whenever the ground-truth controllable latent state is available (which is the case in all of

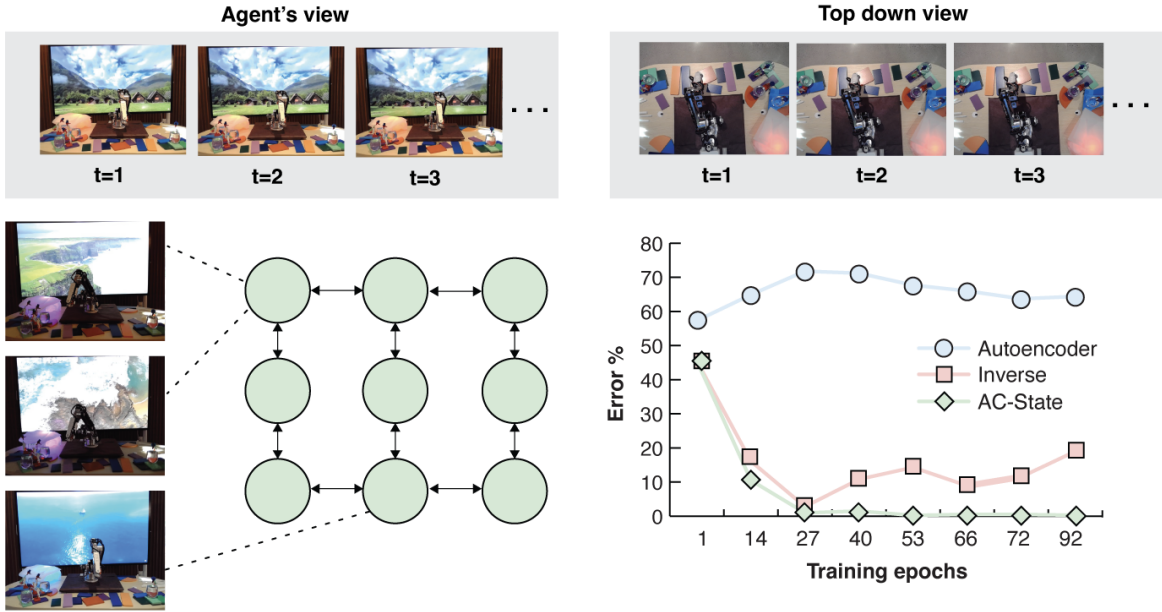


Figure 2: A real robot arm moving between nine positions (left). The quality of controllable latent state dynamics learned by AC-State is better than one-step inverse models and autoencoders (bottom right).

our experiments). We measure an L_1 -error on this dynamics distribution as well as the ratio of the number of learned latent states to the number of ground truth controllable states, which we refer to as *State Parsimony*.

Our experiments explore three domains and demonstrate the unique capabilities of AC-State: (i) AC-State learns the controllable latent state of a real robot from a high-resolution video of the robot with rich temporal background structure (a TV playing a video, flashing lights, dipping birds, and even people) *dominating the information in the observed dynamics*; (ii) multiple mazes and functionally identical agents where only one agent is controlled. AC-State only learns about the controlled agent while ignoring others, enabling the solution of a hard maze-exploration problem. (iii) AC-State learns controllable latent state in a house navigation environment where the observations are high-resolution images and the camera’s vertical position randomly oscillates, showing that AC-State is invariant to exogenous viewpoint noise which radically changes the observation.

We found that AC-State discovers the controllable latent state of a real robot arm, while ignoring distractions. We collected 6 hours of data (14,000 samples) from the robot arm, taking four high level actions (move left, move right, move up, and move down). A picture of the robot was taken after each completed action. The robot was placed with many distractions, such as a television, flashing, color-changing lights, and people moving in the background. Some of these distractions, (especially the TV) had strong temporal correlation between adjacent time steps, as is often the case in real-life situations. We discovered the controllable latent state (Figure 2), which is the ground truth position of the robot (not

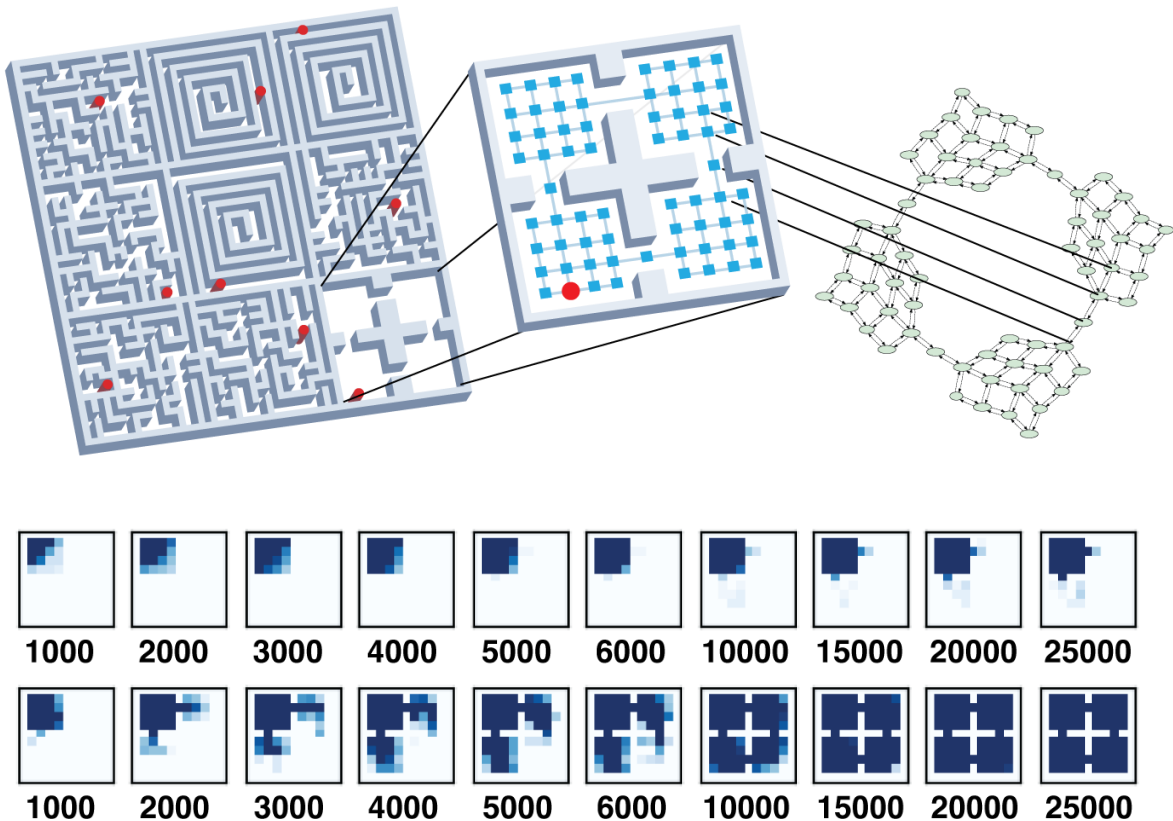


Figure 3: We study a multi-agent world where each of the nine mazes has a separately controlled agent. Training *AC-State* with the actions of a specific agent discovers its controllable latent state while discarding information about the other mazes (top). In a version of this environment where a fixed third of the actions cause the agent’s position to reset to the top left corner, a random policy fails to explore, whereas planned exploration using *AC-State* reaches all parts of the maze (bottom).

used during training). We qualitatively evaluated *AC-State* by training a neural network to reconstruct x from $f(x)$. We found that the robot arm’s position was correctly reconstructed, while the distracting TV and color-changing lights appeared completely blank as expected (Figure 4). As discussed previously, an auto-encoder trained end-to-end with x as input captures both the controllable latent state and distractor noise.

In our experiments, *AC-State* removes exogenous noise in environments where that noise has a rich and complex structure. In particular, we studied a multi-agent system in which a single agent is controllable and the other agents follow their own independent policies. In an environment with 9 agents where each agent has c controllable states, the overall size of the observation space is c^9 . The encoder receives observations of size $80 \times 720 \times 3$ due to the observation from 8 other exogenous agents. The observation is encoded using the MLP-Mixer architecture (24) with gated residual connections (25). The model is trained using the Adam optimizer (26) with the default learning rate of 0.0001 and without

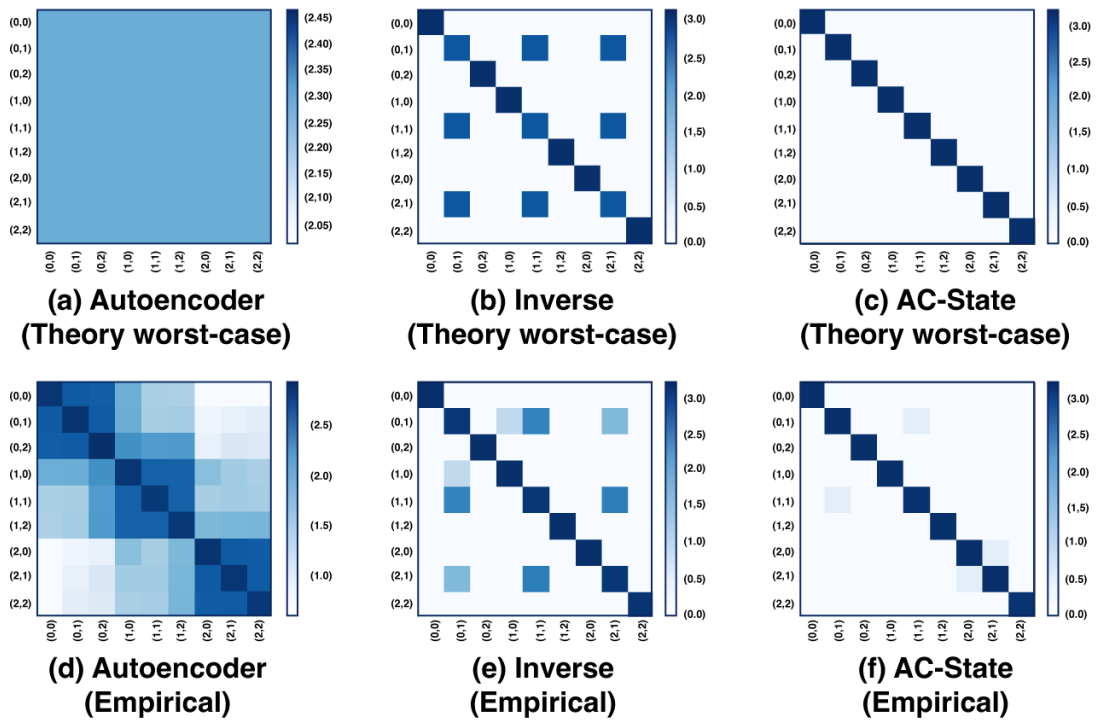


Figure 4: *AC-State* discovers controllable latent state in a visual robotic setting with temporally correlated distractors: a TV, flashing lights, and drinking bird toys (top left). We visualize the learned latent state by training a decoder to reconstruct the observation (top right). This shows that *AC-State* learns to discover the robot arm’s position while ignoring the background distractors (videos in supplement). In co-occurrence histograms (bottom), autoencoders fail (bottom left), one-step inverse models fall prey to the same counterexample in theory and in experiment (bottom center), and *AC-State* discovers a perfect controllable latent state (diagonal histogram, bottom right).

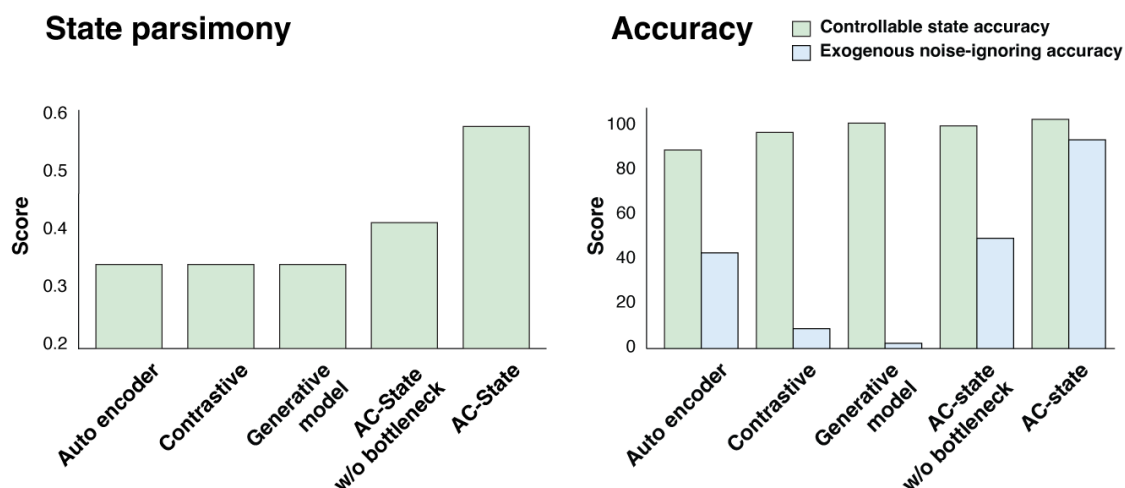
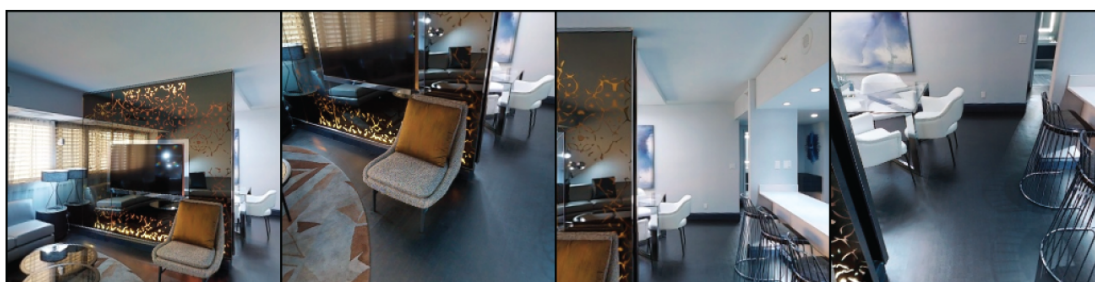
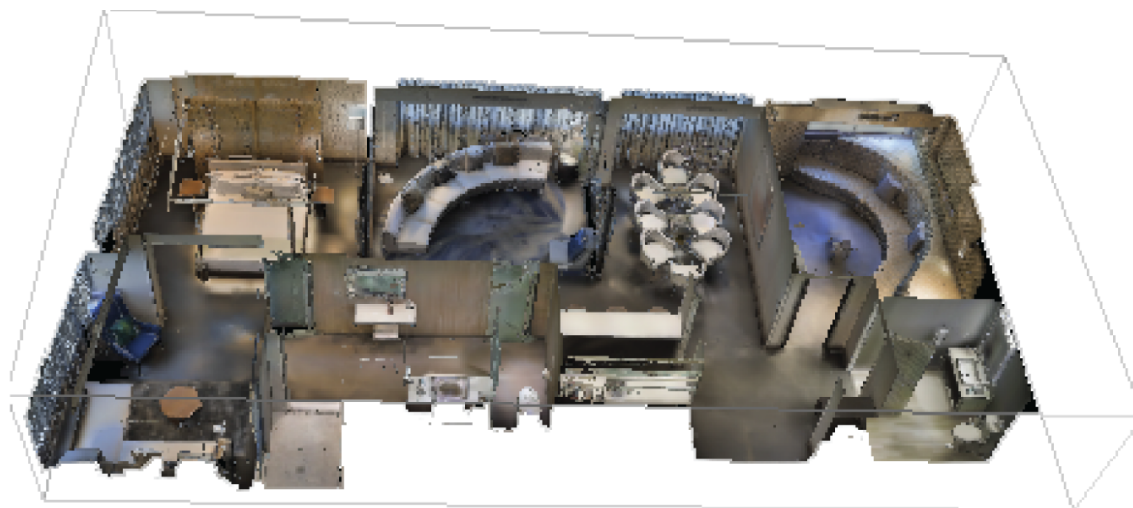


Figure 5: We evaluate AC-State in a house navigation environment (top), where the agent observes high resolution images of first-person views where the vertical position of the camera is random exogenous noise (center). AC-State discovers a controllable latent state which is parsimonious (bottom left). AC-State captures the position of the agent in the house and discards information about the position of the camera (bottom right). The baselines we consider capture the controllable latent state but fail to discard the exogenous noise.

weight decay. With 3,000 training samples, `AC-State` is able to nearly perfectly discover the agent’s controllable latent state, while fully ignoring the state of the 8 uncontrollable exogenous agents with all of the agents controlled by a random policy (Figure 3).

The controllable latent state is useful when it allows for exponentially more efficient exploration than is achievable under a random policy. To exhibit this, we modified the maze problem by giving the agent additional actions which reset to a fixed initial starting position. When a third of all actions cause resets, the probability of acting randomly for N steps without resetting is $(2/3)^N$. We show that a learned exploration policy using `AC-State` succeeds in full exploration and learning of the controllable latent state with 25,000 samples, while a random exploration policy barely explores the first room with the same number of samples (Figure 3).

In order to analyze the performance of the proposed `AC-State` objective in a more realistic setting, we evaluated on Matterport (27), a navigation environment where each observation is a high resolution image taken from a position in a real house. The encoder f is parameterized using a vision transformer (ViT) (28) with four attention heads. We train the model for 20 epochs using Adam optimizer (26) with learning rate $1e-4$. `AC-State` is learned from a dataset with 20,000 samples collected from an agent moving randomly through the house. In addition to the high degree of visual information in the input observations, we randomly move the camera up or down at each step as a controlled source of irrelevant information (exogenous noise). `AC-State` removes view noise from the encoded representation $f(x)$ while still capturing the true controllable latent state (Figure 5) whereas other baselines capture both the controllable latent state and the exogenous noise.

`AC-State` reliably discovers controllable latent state across multiple domains. The vast simplification of the controllable latent state discovered by `AC-State` enables visualization, exact planning, and fast exploration. The field of self-supervised reinforcement learning particularly benefits from these approaches, with `AC-State` useful across a wide range of applications involving interactive agents as a self contained module to improve sample efficiency given any task specification. As the richness of sensors and the ubiquity of computing technologies (such as virtual reality, internet of things, and self-driving cars) continues to grow, the capacity to discover agent-controllable latent states enables new classes of applications.

References

1. Y. LeCun, Y. Bengio, G. Hinton, *Nature* **521**, 436 (2015).
2. Y. Efroni, D. Misra, A. Krishnamurthy, A. Agarwal, J. Langford, *International Conference on Learning Representations* (2022).
3. O. Vinyals, *et al.*, *Nature* **575**, 350 (2019).
4. C. Berner, *et al.*, *arXiv preprint arXiv:1912.06680* (2019).
5. H. Durrant-Whyte, T. Bailey, *IEEE Robotics & Automation Magazine* **13**, 99 (2006).
6. L. Ljung, *Signal Analysis and Prediction* (Springer, 1998), pp. 163–173.
7. C. Cadena, *et al.*, *IEEE Transactions on Robotics* **32**, 1309 (2016).
8. M. G. Dissanayake, P. Newman, S. Clark, H. F. Durrant-Whyte, M. Csorba, *IEEE Transactions on Robotics and Automation* **17**, 229 (2001).
9. I. Goodfellow, Y. Bengio, A. Courville, Y. Bengio, *Deep Learning*, vol. 1 (MIT Press, 2016).
10. T. Wang, *et al.*, *arXiv preprint arXiv:2206.15477* (2022).
11. Z. Wang, X. Xiao, Z. Xu, Y. Zhu, P. Stone, Causal dynamics learning for task-independent state abstraction (2022).
12. Z. D. Guo, *et al.*, *arXiv preprint arXiv:2206.08332* (2022).
13. M. Schwarzer, *et al.*, *Advances in Neural Information Processing Systems 34: Annual Conference on Neural Information Processing Systems 2021, NeurIPS 2021, December 6-14, 2021, virtual*, M. Ranzato, A. Beygelzimer, Y. N. Dauphin, P. Liang, J. W. Vaughan, eds. (2021), pp. 12686–12699.
14. W. Ye, S. Liu, T. Kurutach, P. Abbeel, Y. Gao, *Advances in Neural Information Processing Systems* **34**, 25476 (2021).
15. A. Zhang, R. T. McAllister, R. Calandra, Y. Gal, S. Levine, *International Conference on Learning Representations* (2021).
16. V. Mnih, *et al.*, *Neural Information Processing (NIPS)* .
17. D. Pathak, P. Agrawal, A. A. Efros, T. Darrell, *International conference on machine learning* (PMLR, 2017), pp. 2778–2787.
18. B. Baker, *et al.*, *arXiv preprint arXiv:2206.11795* (2022).
19. A. P. Badia, *et al.*, *International Conference on Machine Learning* (PMLR, 2020), pp. 507–517.
20. M. Hutter, S. Hansen, Uniqueness and complexity of inverse mdp models (2022).
21. H. Bharadhwaj, M. Babaeizadeh, D. Erhan, S. Levine, *International Conference on Learning Representations* (2022).
22. A. A. Alemi, I. Fischer, J. V. Dillon, K. Murphy, *Proceedings of the International Conference on Learning Representations (ICLR)* (2017).

23. A. Van Den Oord, O. Vinyals, *et al.*, *Advances in neural information processing systems* **30** (2017).
24. I. O. Tolstikhin, *et al.*, *Advances in Neural Information Processing Systems, NeurIPS 2021, December 6-14, 2021, virtual* pp. 24261–24272 (2021).
25. E. Jang, S. Gu, B. Poole, *5th International Conference on Learning Representations, ICLR 2017, Toulon, France, April 24-26, 2017, Conference Track Proceedings* (OpenReview.net, 2017).
26. K. Diederik, B. Jimmy, *et al.*, *International Conference on Learning Representations* pp. 273–297 (2014).
27. A. Chang, *et al.*, *International Conference on 3D Vision (3DV)* (2017).
28. A. Dosovitskiy, *et al.*, *International Conference on Learning Representations* (2021).
29. A. van den Oord, O. Vinyals, k. kavukcuoglu, *Advances in Neural Information Processing Systems*, I. Guyon, *et al.*, eds. (Curran Associates, Inc., 2017), vol. 30.
30. A. Vaswani, *et al.*, *Advances in Neural Information Processing Systems* (Curran Associates, Inc., 2017), vol. 30.
31. D. Hendrycks, K. Gimpel, Gaussian Error Linear Units (GELUs) (2016).
32. M. Schwarzer, *et al.*, *9th International Conference on Learning Representations, ICLR 2021, Virtual Event, Austria, May 3-7, 2021* (OpenReview.net, 2021).
33. A. Zhang, R. T. McAllister, R. Calandra, Y. Gal, S. Levine, *9th International Conference on Learning Representations, ICLR 2021, Virtual Event, Austria, May 3-7, 2021* (OpenReview.net, 2021).
34. S. Lange, M. A. Riedmiller, A. Voigtländer, *The 2012 International Joint Conference on Neural Networks (IJCNN), Brisbane, Australia, June 10-15, 2012* (IEEE, 2012), pp. 1–8.
35. N. Wahlström, T. B. Schön, M. P. Deisenroth, *CoRR* **abs/1502.02251** (2015).
36. M. Watter, J. T. Springenberg, J. Boedecker, M. A. Riedmiller, *Advances in Neural Information Processing Systems 28: Annual Conference on Neural Information Processing Systems 2015, December 7-12, 2015, Montreal, Quebec, Canada* (2015), pp. 2746–2754.
37. P. Oudeyer, F. Kaplan, *Frontiers Neurobotics* **1**, 6 (2007).
38. B. C. Stadie, S. Levine, P. Abbeel, *CoRR* **abs/1507.00814** (2015).
39. A. Agarwal, S. M. Kakade, A. Krishnamurthy, W. Sun, *Advances in Neural Information Processing Systems 33: Annual Conference on Neural Information Processing Systems 2020, NeurIPS 2020, December 6-12, 2020, virtual*, H. Larochelle, M. Ranzato, R. Hadsell, M. Balcan, H. Lin, eds. (2020).
40. D. Misra, M. Henaff, A. Krishnamurthy, J. Langford, *International conference on machine learning* (PMLR, 2020), pp. 6961–6971.

41. B. Mazoure, R. T. des Combes, T. Doan, P. Bachman, R. D. Hjelm, *Advances in Neural Information Processing Systems 33: Annual Conference on Neural Information Processing Systems 2020, NeurIPS 2020, December 6-12, 2020, virtual*, H. Larochelle, M. Ranzato, R. Hadsell, M. Balcan, H. Lin, eds. (2020).
42. L. Song, P. Langfelder, S. Horvath, *BMC Bioinform.* **13**, 328 (2012).
43. K. Rakelly, A. Gupta, C. Florensa, S. Levine, *Advances in Neural Information Processing Systems* (Curran Associates, Inc., 2021), vol. 34, pp. 26345–26357.
44. A. S. Klyubin, D. Polani, C. L. Nehaniv, *Advances in Artificial Life*, M. S. Capcarrère, A. A. Freitas, P. J. Bentley, C. G. Johnson, J. Timmis, eds. (Springer Berlin Heidelberg, Berlin, Heidelberg, 2005), pp. 744–753.
45. S. Mohamed, D. J. Rezende, *Advances in Neural Information Processing Systems 28: Annual Conference on Neural Information Processing Systems 2015, December 7-12, 2015, Montreal, Quebec, Canada*, C. Cortes, N. D. Lawrence, D. D. Lee, M. Sugiyama, R. Garnett, eds. (2015), pp. 2125–2133.
46. T. Yu, G. Shevchuk, D. Sadigh, C. Finn, *Robotics: Science and Systems (RSS)* (2019).
47. Y. Efroni, S. Kakade, A. Krishnamurthy, C. Zhang, (*Accepted for publication at International Conference on Machine Learning* (2022)).
48. Y. Efroni, D. J. Foster, D. Misra, A. Krishnamurthy, J. Langford, (*Accepted for publication at Conference on Learning Theory* (2022)).
49. S. Du, *et al.*, *International Conference on Machine Learning* (PMLR, 2019), pp. 1665–1674.
50. D. A. Levin, Y. Peres, *Markov chains and mixing times*, vol. 107 (American Mathematical Soc., 2017).

A Methods and Experiments

In this section, we will describe our methods and experiments for validating the proposed latent state discovery with `AC-State`. Three experiments, in various environments – simulations and physical – are outlined in what follows to test the efficacy of our proposal. The environments are carefully chosen to demonstrate the ability of the `AC-State` agent to succeed at navigation and virtual manipulation tasks with varying degrees of difficulty; on these testbeds, algorithms with similar properties in literature fail to succeed on. In what follows, we will describe the environment setups, function approximation scheme for the latent state, and the results that we produced.

A.1 Mazes with Exogenous Agents and Reset Actions

We consider a global 2D maze (see Fig. 3) further divided into nine 2D maze substructures (henceforth called gridworlds). Each gridworld is made up of 6×6 ground truth states and only one of the gridworlds contains the `AC-State` agent. Every gridworld other than the one containing the true agent has an agent placed within it whose motion is governed by random actions. Our goal is to show that the proposed `AC-State` agent can “discover” the controllable latent state within the global gridworld while ignoring the structural perturbations in the geometry of the other 8 gridworlds.

A.1.1 Exploring Efficiently in Presence of Reset Actions

Data Collection: We collect data under a random roll-out policy while interacting with the gridworlds environment. We endow the agent with an ability to “reset” its action to a fixed starting state. The goal of this experiment is to show that in presence of reset actions, it is sufficiently hard for a random rollout policy to get full coverage of the mazes.

To achieve sufficient coverage we can leverage the discovered controllable latent states to learn a goal seeking policy that can be incentivized to deterministically reach unseen regions of the state space. The counts of the discrete latent states are used to construct a simple tabular MDP where planning is done to reach goal states using a monte carlo version of djikstra’s algorithm (to account for stochastic transition dynamics). The reachable goal states are sampled proportional to $\frac{1}{count(s_i)}$ so that rarely seen states are the most likely to be selected as goals. Experiment results demonstrate that a goal-seeking policy achieves perfect coverage of the state space by using discovered latents for exploration, while a random policy fails to reach more than 25% of the state space, in the presence of reset actions. We demonstrate this with heatmaps showing state visitation frequencies.

Experiment Details : We use a 2 layer feed forward network (FFN) with 512 hidden units for the encoder network, followed by a vector quantization (VQ-VAE) bottleneck. The use of a VQ-VAE bottleneck would discretize the representation from the multi-step inverse model, by adding a codebook of discrete learnable codes. For recovering controllable latents from the maze we want to control, while ignoring the other exogenous mazes, we further use a MLP-Mixer architecture (24) with gated residual updates (25). Both the

inverse mode and the VQ-VAE bottlenecks are updated using an Adam optimizer (26) with default learning rate 0.0001 without weight decay. The agent can receive either abstract observations or pixel based observations of size $80 \times 80 \times 3$. For the multi-maze experiment, the agent receives observation of size $80 \times 720 \times 3$ due to the observation from 8 other exogenous agents. The agent has an action space of 4, where actions are picked randomly from a uniform policy. For the reset action setting, we use an additional 4 reset actions, and uniformly picking a reset action can reset it to a deterministic starting state.

A.2 Matterport Simulator with Exogenous Observations

We evaluated *AC-State* on the matterport simulator introduced in (27). The simulator contains indoor houses in which an agent can navigate. The house contains a finite number of viewpoints which the agent can navigate to. At each viewpoint, the agent has control of its viewing angle (by turning left or right by an angle) and its elevation: in total there are 12 possible viewing angles per viewpoint and 3 possible elevations. We collect data using a random rollout policy. At each step of the rollout policy, the agent navigates to a neighbouring viewpoint. We also randomly change the agent elevation at some of steps of the rollout policy, in order to introduce exogenous information which the agent cannot control. We collect a single long episode of 20,000 state-transitions. The controllable latent state in this setup is the viewpoint information while the exogenous information is the information regarding agent elevation.

Experimental Details The model input is the panorama of the current viewpoint i.e. 12 images for the 12 possible views of each viewpoint. The *AC-State* model f is parameterized using a vision transformer (ViT) (28). Each view within the panorama is fed separately into the ViT as a sequence of patches along with a learnable token called the class (or CLS) following the procedure in (28). To obtain the viewpoint representation, we take the representation corresponding to the CLS token of each view and take the mean across all views. We discretize this representation using a VQ-VAE bottleneck (29) to obtain the final representation. We use a 6-layer transformer with 256 dimensions in the embedding. We use a feedforward network (FFN) after every attention operation in the ViT similar to (30). The FFN is a 2 layer MLP with a GELU activation (31) which first projects the input to a higher dimension D and then projects it back to the original dimension. We set the FFN dimension D to 512. We use 4 heads in the ViT. We train the model for 20 epochs using Adam optimizer (26) with learning rate $1e-4$. The model is trained to predict the viewpoint of the next state as the action.

Results We present the results for this experiment in Figure 5 (right). The *Controllable Latent State Accuracy* is the viewpoint prediction accuracy for the current state. The *Exogenous Noise-Ignoring Accuracy*. is calculate as $1 - \frac{\mathcal{E} - 33.33}{100 - 33.33}$, where \mathcal{E} is elevation prediction accuracy. Thus a higher elevation prediction accuracy leads to a lower the exogenous noise-inducing accuracy. We can see that the proposed *AC-State* model has the highest controllable latent state and exogenous noise-ignoring accuracy. Thus, it outper-

forms the baselines we considered at capturing Controllable Latent State information while ignoring exogenous noise. We calculated state parsimony as $\frac{\text{Num. Ground Truth States}}{\text{Num. Discovered States}}$. Therefore, a lower state parsimony denotes a high number of discovered states which means that the model fails at ignoring exogenous information. The proposed model has the highest state parsimony which shows the effectiveness of the model in ignoring the exogenous noise whilst only capturing controllable latent state.

A.3 Robotic Arm under Exogenous Observations

Using a robot arm with 6 degrees of freedom, with 5 possible abstract actions: forward, reverse, left, right, and stay. The robot arm moves within 9 possible positions in a virtual 3x3 grid, with walls between some cells. The center of each cell is equidistant from adjoining cells. The end-effector is kept at a constant height. We compute the each cell’s centroid and compose a transformation from the joint space of the robot to particular grid cells via standard inverse kinematics calculations.. Two cameras are used to take still images. One camera is facing the front of the robot and the other camera is facing down from above the robot. When a command is received, the robot moves from one cell to the another cell center, assuming no wall is present. After each movement, still images (640x480) are taken from two cameras and appended together into one image (1280x480). During training, only the forward facing, down-sampled (256x256) image is used. Each movement takes one second. After every 500 joint space movements, we re-calibrate the robot to the grid to avoid position drift.

We collected data with the robot arm moving under a uniformly random policy for 6 hours, giving a total of 14000 samples. There were no episodes or state-resets. In addition to the robot, there are several distracting elements in the image. A looped video (<https://www.youtube.com/watch?v=zRpazyH1WzI>) plays on a large display in high resolution (4K video) at 2x speed. Four drinking toy birds, a color changing lamp and flashing streamer lights are also present. During the last half hour of image collection, the distracting elements are moved and/or removed to simulate additional uncertainty in the environment. An illustration of the setup is in Figure 6 along with the specific counter-example for one-step inverse models.

Latent State Visualizations: We learned a visualization of the latent state by learning a small convolutional neural network to map from the latent state $f(x_t)$ to an estimate \hat{x}_t the observation x_t by optimizing the mean-square error reconstruction loss $||\hat{x} - x_t||^2$.

Videos of the latent state visualization for the baseline autoencoder and *AC-State* are included in the supplementary material. In each video, the frontal view (ground truth) is shown on the left, the top-down view (ground truth) is shown in the middle, the reconstruction of the frontal view from the latent state is shown on the right.

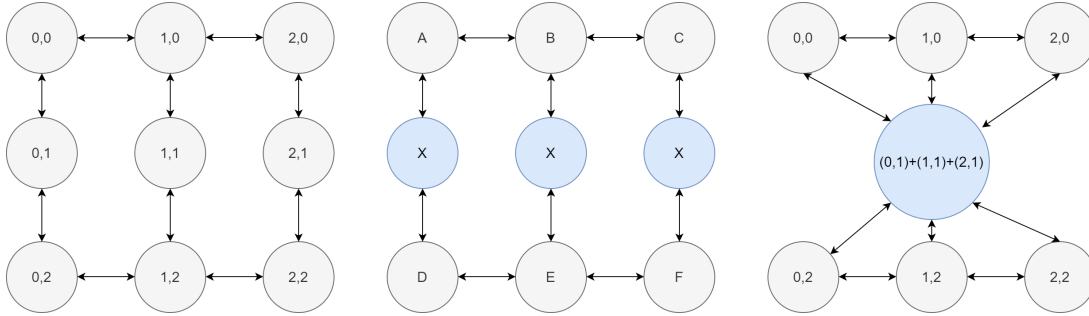


Figure 6: The robot arm has five actions and moves within nine possible controllable states (left). The transition directions are indicated by the arrows. For example, if the robot arm is at $(0,0)$ and selects the down action, it moves to $(0,1)$, but if it selects the up action, it remains at the same position. A simple inverse model can achieve perfect accuracy even if the middle row of true controllable states are mapped to a single latent state (middle), which leads such a model to merge them (right).

B Detailed Related Work

Learning latent states for interactive environments is a mature research area with prolific contributions. We discuss a few of the most important lines of research and how they fail to achieve guaranteed discovery of controllable latent state. We categorize these contributions into three broad areas based around what they predict: latent state prediction, observation prediction, observation-relationship prediction, and action prediction.

Predicting Latent States: In reinforcement learning, learning latent state representations from high dimensional observations consists in maximizing returns to solve a task. Here, a model predicts latent states such that the pre-trained representations can solve a task (32). Deep bisimulation approaches learn state representations for control tasks, under agnosticism to task-irrelevant details (33). An auto-encoder trained with reconstruction loss or a dynamics model, (34–36) learn low-dimensional state representations to capture information relevant for solving a task.

Although learning latent state representations are shown to be useful to solve tasks, there is no guarantee that such methods can fully recover the underlying controllable latent states. The learnt representations capture both controllable and exogenous parts of the latent state, even though the pre-trained representations can be used to solve a task. In contrast, `AC-State` fully recovers the controllable states with a theoretical guarantee, while our experimental results demonstrate that we can fully recover the underlying controllable latent structure, with no dependence on exogenous parts of the state.

Predicting Observations: Prior works have learnt generative models or autoencoders to predict future observations for learning latent representations. This is mostly for exploration. An intrinsic reward signal for exploration in complex domains was achieved by

training an inverse dynamics model to predict actions while also training a dynamics model to predict future observations (17). The idea of predicting observations is often referred to as intrinsic motivation to guide the agent towards exploring unseen regions of the state space (37). Other works use autoencoders to estimate future observations in the feature space for exploration (38), though such models fail in presence of exogenous observations. Dynamics models learn to predict distributions over future observations predictions, but often for planning a sequence of actions, instead of recovering latent states or for purposes of exploration. Theoretically, prior works have learnt representations based on predictive future observations (39), such that the learnt representation is useful for exploration; however, a one step predictive dynamics model is provably forced to capture the exogenous noise (2).

Instead of predicting future observations, AC-State predicts actions based on future observations, and we show that a multi-step inverse dynamics model predicting actions can fully recover the controllable latent states, with no dependence on the exogenous noise. We emphasize that in the presence of exogenous noise, methods based on predictive future observations are prone to predicting both the controllable and exogenous parts of the state space, and do not have guarantees on recovering the latent structure.

Predicting Relation between Observations: By learning to predict relation between two consecutive observations, prior works have attempted at learning latent state representations, both theoretically (40) and empirically (41). By learning representations exploiting mutual information based objectives (information gain based on current states and actions with future states) (41, 42), previous works have attempted at learning controllable states in presence of exogenous noise. However, unlike AC-State, they learn latent states dependent on exogenous noise, even though the learnt representation can be useful for solving complex tasks (41). Theoretically, (40) uses a contrastive loss based objective to provably learn latent state representations that can be useful for hard exploration tasks.

However, contrastive loss based representations can still be prone to exogenous noise (2), whereas AC-State exploits an exogenous free random rollout policy, with a multi-step inverse dynamics model to provably and experimentally recover the full controllable latent state.

Predicting Actions: AC-State aims at recovering the controllable latent states, by training a multi-step inverse dynamics model in presence of exogenous noise. While prior works have explored similar objectives, either for exploration or for learning state representations, they are unable to recover latent states to perfect accuracy in presence of exogenous noise (2). The idea of using a simple one step inverse dynamics models have been explored in the past (17, 21), yet the one step inverse model has counterexamples establishing that it fails to capture the full controllable latent state (2, 20, 40, 43).

Intuitively, the 1-step inverse model is under-constrained and thus may incorrectly merge distinct states which are far apart in the MDP but have a similar local structure. As a simple example, suppose we have a chain of states: $s_1, s_2, s_3, s_4, s_5, s_6$ and $a = 0$ moves earlier in the chain and $a = 1$ moves later in the chain. Suppose s_1, s_3, s_4, s_6 are encoded

as distinct latent states and s_2, s_5 are merged to the same latent state, which we may call s^* . The inverse-model examples containing s^* are: $(s_1, s^*, 1), (s^*, s_1, 0), (s^*, s_3, 1), (s_3, s^*, 0), (s_4, s^*, 1), (s^*, s_4, 0), (s^*, s_6, 1), (s_6, s^*, 0)$. Because all of these examples have distinct inputs, 1-step inverse model still has zero error despite the incorrect merger of the states s_2 and s_5 .

Empowerment based objectives focus on the idea that an agent should try to seek out states where it is empowered by having the greatest number of possible states which it can easily reach (44). For example, in a maze with two rooms, the most empowered state is in the doorway, since it makes it easy to reach either of the rooms. Concrete instantiations of the empowerment objective may involve training models to predict the distribution over actions from observations (either single-step or multi-step inverse models) (45,46), but lack the information bottleneck term and the requirement of an exogenous-independent rollout policy. The analysis and theory in this work focuses on action-prediction as a particular method for measuring empowerment, rather than as a way of guaranteeing discovery of a minimal controllable latent state and ignoring exogenous noise.

In contrast, *AC-State* uses a simple multi-step inverse dynamics model, with an exogenous-independent (for example, random) rollout policy, and provably guarantees perfect recovery of only the controllable part of the state space, in presence of exogenous noise, either from other agents acting randomly in the environment, or in presence of background distractors. We emphasize the simplicity of *AC-State* to use a simple inverse dynamics model to learn latent states, which has not been exploited by prior works using dynamics models.

Provable reinforcement learning and control in the presence of exogenous noise.

Here we discuss on several recent works that study the reinforcement learning problem in the presence of exogenous and irrelevant information.

In (2) the authors formulated the Ex-BMDP model and designed a provably efficient algorithm that learns the state representation. However, their algorithm succeeds only in the episodic setting, when the initial controllable state is initialized deterministically. This strict assumption makes their algorithm impractical in many cases of interest. Here we removed the deterministic assumption of the initial latent state. Indeed, as our theory suggests, *AC-State* can be applied in the you-only-leave-once setting, when an agent has access to a single trajectory.

In (47, 48) the authors designed provable RL algorithms that efficiently learn in the presence of exogenous noise under different assumptions on the underlying dynamics. These works, however, focused on statistical aspects of the problem; how to scale these approaches to complex environments and combine function approximations is currently unknown and seems challenging.

Unlike the aforementioned works, here we focus on the representation learning problem. Our goal is to design a practical and guaranteed approach by which we can learn the controllable representation with complex function approximators such as deep neural networks. Our algorithm, *AC-State*, is the first algorithm that achieves this task.

C Analysis and Discussion

C.1 High-Level Overview of Theory

We present asymptotic analysis of *AC-State* showing it recovers f_* , the controllable latent state representation. The mathematical model we consider is the deterministic Ex-BMDP. There, the transition model of the latent state decomposes into a controllable latent state, which evolves deterministically, along with a noise term—the uncontrollable portion of the state. The noise term may be an arbitrary temporally correlated stochastic process. If the reward does not depend on this noise, any optimal policy may be expressed in terms of this controllable latent state. In this sense, the recovered controllable latent state is sufficient for achieving optimal behavior.

Intuitively, the Ex-BMDP is similar to a video game, in which a “game engine” takes player actions and keeps track of an internal game state (the controllable state component), while the visuals and sound are rendered as a function of this compact game state. A modern video game’s core state is often orders of magnitude smaller than the overall game.

The algorithm we propose for recovering the optimal controllable latent state involves (i) an action prediction term; and (ii) a mutual information minimization term. The action prediction term forces the learned representation $\hat{f}(x)$ to capture information about the dynamics of the system. At the same time, this representation for $\hat{f}(x)$ (which is optimal for action-prediction) may also capture information which is unnecessary for control. In our analysis we assume that $\hat{f}(x)$ has discrete values and show the controllable latent state is the unique coarsest solution.

To enable more widespread adoption in deep learning applications, we can generalize this notion of coarseness to minimizing mutual information between x and $f(x)$. These are related by the data-processing inequality; coarser representation reduces mutual information with the input. Similarly, the notion of mutual information is general as it does not require discrete representation.

C.2 Preliminaries

We consider the Exogenous Block Markov Decision Process (Ex-BMDP) setting to model systems with exogenous and irrelevant noise components as formulated in (2). We first formalize the Block Markov Decision Process (BMDP) model (49).

A BMDP consists of a finite set of observations, \mathcal{X} ; a set of latent states, \mathcal{Z} with cardinality Z ; a finite set of actions, \mathcal{A} with cardinality A ; a transition function, $T : \mathcal{Z} \times \mathcal{A} \rightarrow \Delta(\mathcal{Z})$; an emission function $q : \mathcal{Z} \rightarrow \Delta(\mathcal{X})$; a reward function $R : \mathcal{X} \times \mathcal{A} \rightarrow [0, 1]$; and a start state distribution $\mu_0 \in \Delta(\mathcal{Z})$. The agent interacts with the environment, generating a single trajectory of latent state, observation and action sequence, $(z_1, x_1, a_1, z_2, x_2, a_2, \dots)$, where $z_1 \sim \mu_0$ we have $x_t \sim q(\cdot | z_t)$. The agent does not observe the latent states (z_1, z_2, \dots) , instead it receives only the observations (x_1, x_2, \dots) . The block assumption holds if the support of the emission distributions of any two latent states are disjoint,

$$\text{supp}(q(\cdot | z_1)) \cap \text{supp}(q(\cdot | z_2)) = \emptyset \text{ when } z_1 \neq z_2.,$$

where $\text{supp}(q(\cdot | z)) = \{x \in \mathcal{X} \mid q(x | z) > 0\}$ for any latent state z . Lastly, the agent chooses actions using a policy $\pi : \mathcal{X} \rightarrow \Delta(\mathcal{A})$.

We now define the model we consider in this work, which we refer as deterministic Ex-BMDP.

Definition 1 (Deterministic Ex-BMDP). *A deterministic Ex-BMDP is a BMDP such that the latent state can be decoupled into two parts $z = (s, e)$ where $s \in \mathcal{S}$ is the controllable state and $e \in \Xi$ is the exogenous state. For $z, z' \in \mathcal{Z}, a \in \mathcal{A}$ the transition function is decoupled $T(z' | z, a) = T(s' | s, a)T_e(e' | e)$.*

The above definition implies that there exists mappings $f_* : \mathcal{X} \rightarrow [S]$ and $f_{*,e} : \mathcal{X} \rightarrow [E]$ from observations to the corresponding controllable and exogenous latent states. Further, E , the cardinality of the exogenous latent state may be arbitrarily large.

Observe that we do not consider the episodic setting, but only assume access to a single trajectory.

Furthermore, we assume that the diameter of the controllable part of the state space is bounded. We make the following assumption.

Assumption 2 (Bounded Diameter of Controllable State Space). *The length of the shortest path between any $z_1 \in \mathcal{S}$ to any $z_2 \in \mathcal{S}$ is bounded by D .*

We now describe a structural result of the Ex-BMDP model, proved in (2). We say that $\pi : \mathcal{X} \rightarrow \Delta(\mathcal{A})$ is an endogenous policy if it is not a function of the exogenous noise. Formally, for any x_1 and x_2 , if $f_*(x_1) = f_*(x_2)$ then $\pi(\cdot | x) = \pi(\cdot | f_*(x))$.

Denote by $\mathbb{P}_\pi(f_*(x') | f_*(x), t)$ as the probability to observe the controllable latent state $s = f_*(x')$ t time steps after observing $s' = f_*(x)$ and following policy π . The following result shows that, when executing an endogenous policy, the future t time step distribution of the observation process conditioning on any x has a decoupling property. Using this decoupling property we will later prove that the controllable state partition is sufficient to represent the action-prediction model.

Proposition 3 (Factorization Property of Endogenous Policy, (2), Proposition 3). *Assume that $x \sim \mu(x)$ where μ is some distribution over the observation space and that π is an endogenous policy. Then, for any $t \geq 1$ it holds that*

$$\mathbb{P}_\pi(x' | x, t) = q(x' | f_*(x'), f_{*,e}(x')) \mathbb{P}_\pi(f_*(x') | f_*(x), t) \mathbb{P}(f_{*,e}(x') | f_{*,e}(x), t).$$

Observe that the assumptions used in (2) are two-fold; that π is an endogenous policy, and that the initial distribution at time step $t = 0$ is decoupled $\mu_0(s, e) = \mu_0(s)\mu_0(e)$. In our case, we condition on x , the initial observation. This also implies that the latent state at the initial time step is deterministic, and, hence, the initial distribution is decoupled $\mu_0(s, e) = 1 \{s = f^*(x)\} 1 \{e = f_e^*(x)\}$. Hence, the result of (2) is also applicable in our you-only-live-once setting.

C.3 The Controllable Partition is a Bayes' Optimal Solution

Consider the generative process in which x is sampled from a distribution μ , the agent executes a policy π for t time steps and samples x' . Denote by $\mathbb{P}_{\pi,\mu}(x, x', t)$ as the joint probability, and by $\mathbb{P}_{\pi,\mu}(a | x, x', t)$ as the probability that under this generative process the action upon observing x is a . The following result, which builds on Proposition 3, shows that the optimal bayes solution $\mathbb{P}_{\pi,\mu}(a | x, x', t)$ is equal to $\mathbb{P}_{\pi,\mu}(a | f_\star(x), f_\star(x'), t)$ for $\mathbb{P}_{\pi,\mu}(x, x', t) > 0$, where $\mathbb{P}_{\pi,\mu}(x, x', t) > 0$ is the probability to sample x .

Proposition 4. *Assume that π is an endogenous policy. Let $x \sim \mu$ for some distribution μ . Then, the Bayes' optimal predictor of the action-prediction model is piece-wise constant with respect to the controllable partition: for all $a \in \mathcal{A}$, $t > 0$ and $x, x' \in \mathcal{X}$ such that $\mathbb{P}_{\pi,\mu}(x, x', t) > 0$ it holds that*

$$\mathbb{P}_{\pi,\mu}(a | x, x', t) = \mathbb{P}_{\pi,\mu}(a | f_\star(x), f_\star(x'), t).$$

We comment that the condition $\mathbb{P}_{\pi,\mu}(x, x', t) > 0$ is necessary since, otherwise, the conditional probability $\mathbb{P}_{\pi,\mu}(a | x, x', t)$ is well not defined.

Proposition 4 is readily proved via the factorization of the future observation distribution to controllable and exogenous parts that holds when the executed policy does not depend on the exogenous state (Proposition 3).

Proof. The proof follows by applying Bayes' theorem, Proposition (3), and eliminating terms from the numerator and denominator.

Fix any $t > 0$, $x, x' \in \mathcal{X}$ and $a \in \mathcal{A}$ such that $\mathbb{P}_{\pi,\mu}(x', x, t) > 0$. The following relations hold.

$$\begin{aligned} & \mathbb{P}_{\pi,\mu}(a | x', x, t) \\ & \stackrel{(a)}{=} \frac{\mathbb{P}_{\pi,\mu}(x' | x, a, t) \mathbb{P}_{\pi,\mu}(a | x)}{\sum_{a'} \mathbb{P}_{\pi,\mu}(x' | x, a', t)} \\ & \stackrel{(b)}{=} \frac{\mathbb{P}_{\pi,\mu}(x' | x, a, t) \pi(a | f_\star(x))}{\sum_{a'} \mathbb{P}_{\pi,\mu}(x' | x, a', t) \pi(a' | f_\star(x))} \\ & \stackrel{(c)}{=} \frac{q(x' | f_\star(x'), f_{\star,e}(x')) \mathbb{P}_{\pi,\mu}(f_\star(x') | f_\star(x), a, t) \mathbb{P}_{\pi,\mu}(f_{\star,e}(x') | f_{\star,e}(x), t) \pi(a | f_\star(x))}{\sum_{a'} q(x' | f_\star(x'), f_{\star,e}(x')) \mathbb{P}_{\pi,\mu}(f_\star(x') | f_\star(x), a', t) \mathbb{P}_{\pi,\mu}(f_{\star,e}(x') | f_{\star,e}(x), t) \pi(a' | f_\star(x))} \\ & = \frac{\mathbb{P}_{\pi,\mu}(f_\star(x') | f_\star(x), a, t) \pi(a | f_\star(x))}{\sum_{a'} \mathbb{P}_{\pi,\mu}(f_\star(x') | f_\star(x), a', t) \pi(a' | f_\star(x))}. \end{aligned}$$

Relation (a) holds by Bayes' theorem. Relation (b) holds by the assumption that π is endogenous. Relation (c) holds by Proposition (3).

Thus, $\mathbb{P}_{\pi,\mu}(a | x', x, t) = \mathbb{P}_{\pi,\mu}(a | f_\star(x'), f_\star(x), t)$, and is constant upon changing the observation while fixing the controllable latent state. \square

C.4 The Coarsest Partition is the Controllable State Partition

Proposition 4 from previous section shows that the multi-step action-prediction model is piece-wise constant with respect to the partition induced by the controllable states $f_\star : \mathcal{X} \rightarrow [S]$.

In this section, we assume that the executed policy is an endogenous policy that induces sufficient exploration. With this, we prove that there is no coarser partition of the observation space such that the set of inverse models are piece-wise constant with respect to it.

We make the following assumptions on the policy by which the data is collected.

Assumption 5. *Let $T_{\mathcal{D}}(s' | s)$ be the Markov chain induced on the controllable state space by executing the policy $\pi_{\mathcal{D}}$ by which AC-State collects the data.*

1. *The Markov chain $T_{\mathcal{D}}$ has a stationary distribution $\mu_{\mathcal{D}}$ such that $\mu_{\mathcal{D}}(s, a) > 0$ and $\pi_{\mathcal{D}}(a | s) \geq \pi_{\min}$ for all $s \in \mathcal{S}$ and $a \in \mathcal{A}$.*
2. *The policy $\pi_{\mathcal{D}}$ by which the data is collected reaches all accessible states from any states. For any $s, s' \in \mathcal{S}$ and any $h > 0$ if s' is reachable from s then $\mathbb{P}_{\mathcal{D}}(s' | s, h) > 0$.*
3. *The policy $\pi_{\mathcal{D}}$ does not depend on the exogenous state, and is an endogenous policy.*

See (50), Chapter 1, for further discussion on the classes of Markov chains for which the assumption on the stationary distribution hold. The second and third assumptions are satisfied for the the random policy that simply executes random actions.

We consider the stochastic process in which an observation is sampled from a distribution μ such that $\mu(s) = \mu_{\mathcal{D}}(s)$ for all s . Then, the agent executes the policy $\pi_{\mathcal{D}}$ for t time steps. For brevity, we denote the probability measure induced by this process as $\mathbb{P}_{\mathcal{D}}$.

We begin by defining several useful notions. We denote the set of reachable controllable states from s in h time steps as $\mathcal{R}_h(s)$.

Definition 6 (Reachable Controllable States). *Let the set of reachable controllable states from $s \in \mathcal{S}$ in $h > 0$ time steps be $\mathcal{R}(s, h) = \{s' | \max_{\pi} \mathbb{P}_{\pi}(s' | s, h) = 1\}$.*

Observe that every reachable state from s in h time steps satisfies that $\max_{\pi} \mathbb{P}_{\pi, \mu}(s' | s_0 = s, h) = 1$ due to the deterministic assumption of the controllable dynamics.

Next, we define a notion of consistent partition with respect to a set of function values. Intuitively, a partition of space \mathcal{X} is consistent with a set of function values if the function is piece-wise constant on that partition.

Definition 7 (Consistent Partition with respect to \mathcal{G}). *Consider a set $\mathcal{G} = \{g(a, y, y')\}_{y, y' \in \mathcal{Y}, a \in \mathcal{A}}$ where $g : \mathcal{A} \times \mathcal{Y} \times \mathcal{Y} \rightarrow [0, 1]$. We say that $f : \mathcal{Y} \rightarrow [N]$ is a consistent partition with respect to \mathcal{G} if for all $y, y'_1, y'_2 \in \mathcal{Y}$ $f(y'_1) = f(y'_2)$ implies that $g(a, y, y'_1) = g(a, y, y'_2)$ for all $a \in \mathcal{A}$.*

Observe that Proposition 4 shows that the partition of \mathcal{X} according to f_{\star} is consistent with respect to $\{\mathbb{P}_{\mathcal{D}}(a | x, x', h) | x, x' \in \mathcal{X}, h \in [H] \text{ s.t. } \mathbb{P}_{\mathcal{D}}(x, x', h) > 0\}$, since, by Proposition 4, $\mathbb{P}_{\mathcal{D}}(a | x, x', h) = \mathbb{P}_{\mathcal{D}}(a | f_{\star}(x), f_{\star}(x'), h)$.

Towards establishing that the coarsest abstraction according to the AC-State objective is f_{\star} we make the following definition.

Definition 8 (The Generalized Inverse Dynamics Set $\text{AC}(s, h)$). *Let $s \in \mathcal{S}, h \in \mathbb{N}$. We denote by $\text{AC}(s, h)$ as the set of multi-step inverse models accessible from s in h time steps. Formally,*

$$\text{AC}(s, h) = \{\mathbb{P}_{\mathcal{D}}(a | s', s'', h') : s' \in \mathcal{R}(s, h - h'), s'' \in \mathcal{R}(s', h'), a \in \mathcal{A}, h' \in [h]\}. \quad (4)$$

Observe that in equation (4) the inverse function $\mathbb{P}_{\mathcal{D}}(a \mid s', s'', h')$ is always well defined since $\mathbb{P}_{\mathcal{D}}(s', s'', h') > 0$. It holds that

$$\mathbb{P}_{\mathcal{D}}(s', s'', h') = \mathbb{P}_{\mathcal{D}}(s')\mathbb{P}_{\mathcal{D}}(s'' \mid s', h') > 0,$$

since $\mathbb{P}_{\mathcal{D}}(s') > 0$ and $\mathbb{P}_{\mathcal{D}}(s'' \mid s', h') > 0$. The inequality $\mathbb{P}_{\mathcal{D}}(s') > 0$ holds by the assumption that the stationary distribution when following \mathcal{U} has positive support on all controllable states (Assumption 5). The inequality $\mathbb{P}_{\mathcal{D}}(s'' \mid s', h') > 0$ holds since, by definition $s'' \in \mathcal{R}(s, h')$ is reachable from s' in h' time steps; hence, $\mathbb{P}_{\mathcal{D}}(s'' \mid s', h') > 0$ by the fact that Assumption 5 implies that the policy $\pi_{\mathcal{D}}$ induces sufficient exploration.

Theorem 9 (f_{\star} is the coarsest partition consistent with AC-State objective). *Assume 2 and 5 holds. Then there is no coarser partition than f_{\star} which is consistent with $\text{AC}(s, D)$ for any $s \in \mathcal{S}$.*

Proof. We will show inductively that for any $h > 0$ and $s \in \mathcal{S}$ there is no coarser partition than $\mathcal{R}(s, h)$ for the set $\mathcal{R}(s, h)$ that is consistent with $\text{AC}(s, h)$. Since the set of reachable states in $h = D$ time steps is \mathcal{S} —all states are reachable from any state in D time steps—it will directly imply that there is no coarser partition than $\mathcal{R}(s, D) = \mathcal{S}$ consistent $\text{AC}(s, D)$.

Base case, $h = 1$. Assume that $h = 1$ and fix some $s \in \mathcal{S}$. Since the controllable dynamics is deterministic, there are A reachable states from s . Observe the inverse dynamics for any $s' \in \mathcal{R}(s, 1)$ satisfies that

$$\mathbb{P}_{\mathcal{D}}(a \mid s, s', 1) = \begin{cases} 1 & \text{if } a \text{ leads } s' \text{ from } s \\ 0 & \text{o.w.} \end{cases}. \quad (5)$$

This can be proved by an application of Bayes' rule:

$$\begin{aligned} \mathbb{P}_{\mathcal{D}}(a \mid s, s', 1) &= \frac{\mathbb{P}_{\mathcal{D}}(s' \mid s = s, a, 1)\pi_{\mathcal{D}}(a \mid s)}{\sum_{a'} \mathbb{P}_{\mathcal{D}}(s' \mid s = s, a', 1)\pi_{\mathcal{D}}(a' \mid s)} \\ &= \frac{T(s' \mid s, a)\pi_{\mathcal{D}}(a \mid s)}{\sum_{a'} T(s' \mid s, a')\pi_{\mathcal{D}}(a' \mid s)} \\ &\begin{cases} \geq \pi_{\min} & (s, a) \text{ leads to } s' \\ = 0 & \text{o.w.} \end{cases}, \end{aligned}$$

where the last relation holds by Assumption 5. Furthermore, observe that since $s' \in \mathcal{R}(s, 1)$, i.e., it is reachable from s , the probability function $\mathbb{P}_{\mathcal{D}}(a \mid s, s', 1)$ is well defined.

Hence, by equation (5), we get that for any $s'_1, s'_2 \in \mathcal{R}(s, 1)$ such that $s'_1 \neq s'_2$ it holds that exists $a \in \mathcal{A}$ such that

$$\pi_{\min} \geq \mathbb{P}_{\mathcal{D}}(a \mid s, s'_1, 1) \neq \mathbb{P}_{\mathcal{D}}(a \mid s, s'_2, 1) = 0.$$

Specifically, choose a such that taking a from s leads to s'_1 and see that, by equation (5),

$$\pi_{\min} \geq \mathbb{P}_{\mathcal{D}}(a \mid s, s'_1, 1) \neq \mathbb{P}_{\mathcal{D}}(a \mid s, s'_2, 1) = 0.$$

Lastly, by the fact that $s \in \mathcal{S}$ is an arbitrary state, the induction base case is proved for all $s \in \mathcal{S}$.

Induction step. Assume the induction claim holds for all $t \in [h]$ where $h \in \mathbb{N}$. We now prove it holds for $t = h + 1$.

Fix some $s \in \mathcal{S}$. We prove the induction step and show that $\mathcal{R}(s, h + 1)$ is the coarsest partition which is consistent AC($s, h + 1$). Meaning, there exists $\bar{s}, t \in [h + 1]$, a such that $\mathbb{P}(a \mid \bar{s}, s'_1, 1), \mathbb{P}(a \mid \bar{s}, s'_1, 1) \in \text{AC}(\bar{s}, h + 1)$ and

$$\mathbb{P}_{\mathcal{D}}(a \mid \bar{s}, s'_1, t) \neq \mathbb{P}_{\mathcal{D}}(a \mid \bar{s}, s'_2, t). \quad (6)$$

Observe that, by Definition 8, it holds that,

$$\text{AC}(s, h + 1) = \{\mathbb{P}_{\mathcal{D}}(a \mid s, s', h + 1)\}_{s' \in \mathcal{R}(s, h + 1)} \cup_{\bar{s} \in \mathcal{R}(s, 1)} \text{AC}(\bar{s}, h).$$

Meaning, the set $\text{AC}(s, h + 1)$ can be written as the union of (1) the set $\{\mathbb{P}_{\mathcal{D}}(a \mid s, s', h + 1)\}_{s' \in \mathcal{R}(s, h + 1)}$, and (2) the union of the sets $\text{AC}(\bar{s}, h)$ for all \bar{s} which is reachable from s in a single time step.

By the induction hypothesis, the coarsest partition which is consistent with $\text{AC}(\bar{s}, h)$ is $\cup_{h'=1}^h \mathcal{R}(\bar{s}, h')$. We only need to prove, that for any $\bar{s}_1, \bar{s}_2 \in \mathcal{R}(s, h + 1)$ such that $\bar{s}_1 \neq \bar{s}_2$ exists some $a \in \mathcal{A}, h' \in [h]$ and $s_{h'} \in \mathcal{R}(s, h + 1)$ such that

$$\mathbb{P}_{\mathcal{D}}(a \mid s_{h'}, \bar{s}_1, h') \neq \mathbb{P}_{\mathcal{D}}(a \mid s_{h'}, \bar{s}_2, h'),$$

this will imply that the set of reachable states in $h + 1$ time states is also the coarsest partition which is consistent with $\text{AC}(s, h + 1)$.

Fix $\bar{s}_1, \bar{s}_2 \in \mathcal{R}(s, h + 1)$ such that $\bar{s}_1 \neq \bar{s}_2$ we show that exists a certificate in $\text{AC}(s, h + 1)$ that differentiate between the two by considering three cases.

1. **Case 1:** Both \bar{s}_1 and \bar{s}_2 are reachable from all $s' \in \mathcal{R}(s, 1)$. In this case, for all $s' \in \mathcal{R}(s, 1)$ it holds that $\bar{s}_1, \bar{s}_2 \in \mathcal{R}(s', h)$. By the induction hypothesis, \bar{s}_1 and \bar{s}_2 cannot be merged while being consistent with $\text{AC}(s', h)$.
2. **Case 2:** Exists $s' \in \mathcal{R}(s, 1)$ such \bar{s}_1 is reachable from s' in h time steps and \bar{s}_2 is not. Let a be the action that leads to s' from state s . In that case, it holds by the third assumption of Assumption 5 that

$$\begin{aligned} \mathbb{P}_{\mathcal{D}}(a \mid s, \bar{s}_1, h + 1) &\stackrel{(a)}{=} \frac{\mathbb{P}_{\mathcal{D}}(\bar{s}_1 \mid s, a, h + 1)\pi_{\mathcal{D}}(a \mid s)}{\sum_{a'} \mathbb{P}_{\mathcal{D}}(\bar{s}_1 \mid s, a', h + 1)\pi_{\mathcal{D}}(a' \mid s)} \\ &\stackrel{(b)}{=} \frac{\mathbb{P}_{\mathcal{D}}(\bar{s}_1 \mid s', h)\pi_{\mathcal{D}}(a \mid s)}{\sum_{a'} \mathbb{P}_{\mathcal{D}}(\bar{s}_1 \mid s, a', h + 1)\pi_{\mathcal{D}}(a' \mid s)} \\ &\stackrel{(c)}{\geq} \pi_{\min} \frac{\mathbb{P}_{\mathcal{D}}(\bar{s}_1 \mid s', h)}{\sum_{a'} \mathbb{P}_{\mathcal{D}}(\bar{s}_1 \mid s, a', h + 1)} \\ &\stackrel{(d)}{>} 0. \end{aligned} \quad (7)$$

Relation (a) holds by Bayes' rule. Relation (b) holds by the fact that (s, a) deterministically leads to s' . Relation (c) and (d) holds by Assumption 5.

Observe that $\mathbb{P}_{\mathcal{D}}(a \mid s, \bar{s}_2, h + 1) = 0$ since \bar{s}_2 is not reachable upon taking action a from state s , by the assumption. Combining this fact with equation (7) implies that

$$0 < \mathbb{P}_{\mathcal{D}}(a \mid s, \bar{s}_1, h + 1) \neq \mathbb{P}_{\mathcal{D}}(a \mid s, \bar{s}_2, h + 1) = 0.$$

Hence, exists a certificate that differentiates between \bar{s}_1 and \bar{s}_2 . Observe that since $\bar{s}_2 \in \mathcal{R}(s, h + 1)$, i.e., it is reachable from s , it holds that $\mathbb{P}_{\mathcal{D}}(a \mid s, \bar{s}_2, h + 1) = 0$, i.e., it is well defined.

3. **Case 3:** Exists $s' \in \mathcal{R}(s, 1)$ such \bar{s}_2 is reachable from s' in h time steps and \bar{s}_1 is not. Symmetric to case 2.

This establishes the result we needed to show in equation (6) and, hence, the induction and result hold. \square

C.5 Reinforcement Learning with Rewards

Our theory has discussed the case where we want to learn a representation $f(x)$ in the absence of reward or other supervision. If the reward is only a function of the controllable latent state, then the $f(x)$ learned with *AC-State* is fully sufficient for reinforcement learning using that reward signal. If the reward depends on both the controllable latent state and the exogenous noise, but with an additive relationship, then *AC-State* is sufficient for learning the optimal policy but may lead to incorrect learning of the value-function. In the case where reward depends on both the controllable latent state and exogenous noise, with a non-linear interaction, then *AC-State* would need to be modified to have $f(x_t)$ also predict rewards. Intuitively, if we think about the robot-arm control problem with a distracting background TV, we could consider a case where reward is given when the robot is to the left and the TV shows a specific frame. In this case, our controllable latent state needs to be made less coarse to also capture the reward information in its latent state.

At the same time, learning from rewards is insufficient for learning the controllable latent state, as we could imagine a setting where two controllable latent states are equivalent from the perspective of the value function yet are distinct states.